Journal of Materials Chemistry A

Accepted Manuscript

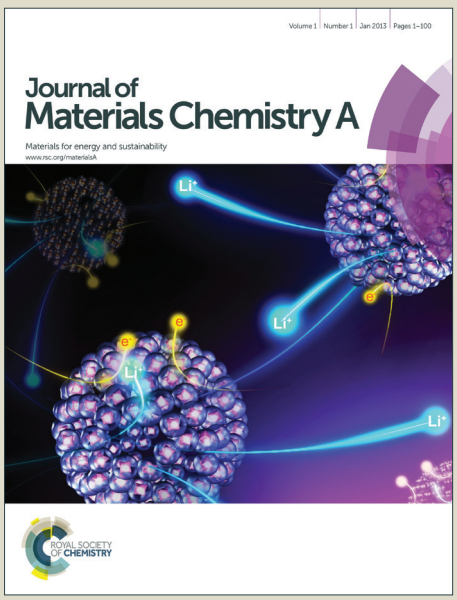

ROYAL SOCIETY OF CHEMISTRY

www.rsc.org/materialsA

Journal of Materials Chemistry A

Dynamic Article Links ►

Cite this: DOI: 10.1039/c0xx00000x

ARTICLE TYPE

www.rsc.org/xxxxxx

Sulfonated Polyimide and PVDF Based Blend Proton Exchange Membranes for Fuel Cell Applications

Qin Yuan,*[a,b] Ping Liu[a,c] and Gregory L. Baker[a,d]

Received (in XXX, XXX) Xth XXXXXXXXX 20XX, Accepted Xth XXXXXXXXX 20XX

DOI: 10.1039/b000000x

Sulfonated polyimide (SPI) is synthesized by a polycondensation reaction and proton exchange membranes (PEMs) are prepared from the SPI/Poly(vinylidene fluoride) (PVDF) blends. Compared to commercial Nafion, the SPI/PVDF blend PEMs have significantly improved swelling ratio of <3 % (vs. ~18 % for Nafion), as well as high proton conductivity of 75 mS/cm for 50 wt% of SPI content (vs. ~62 mS/cm for Nafion). The proton conducting mechanism in blend membrane was studied and dramatic increases in proton conductivity and water uptake at ~30 wt% SPI were observed, which are proved by TEM to be due to the transition from isolated SPI ionic domains in PVDF matrix to a bi-continuous morphology - a percolation phenomenon.

Introduction

Recently, there has been considerable interest in the development of fuel cells, especially hydrogen powered fuel cells, which cleanly convert the chemical energy of fuels directly into electric energy and heat with high efficiency. A key component of hydrogen based fuel cells is the proton exchange membrane (PEM), which transports protons from the anode to the cathode and separates fuels and the oxidant. Nafion, the prototype PEM, has high proton conductivity and excellent chemical and mechanical stability at moderate temperatures in the harsh fuel cell environment. Although the actual morphology of hydrated Nafion is still under investigation, it's widely agreed that microphase-separation of Nafion's perfluorocarbon backbone and pendent perfluorosulfonic acid groups accounts for its high proton conductivity.[1-4] The two domains of Nafion provide separate properties: the hydrophilic domain supports efficient proton transport while the hydrophobic domain provides mechanical and chemical stability. Despite the high performance of Nafion in fuel cells, its high manufacturing cost, drastically reduced proton conductivity above 80 ºC, environmental incompatibility, and severe methanol permeability limit its use in fuel cell applications.[4]

Developing alternatives to Nafion, especially those that can operate at high temperatures, is a major challenge in current fuel cell research. The usual design strategy for such membranes has been to synthesize sulfonated analogues of thermally stable polymers, such as sulfonated poly(arylene ether ether ketone),[3,5] sulfonated polyimides,[6-8] sulfonated polysulfone,[9-11] and sulfonated polystyrene.[12-13] Membranes derived from these polymers have advantages over Nafion in terms of cost and reduced methanol cross-over, but in their hydrated state, they generally suffer from poor dimensional, chemical, and mechanical stability.[14-18] The problems associated with sulfonated polymers can be overcome by the use of polymer blends, which are comprised of a hydrophilic polyelectrolyte phase-embedded in a non-conductive material for reinforcement.

The two components of a blend membrane provide complementary functions: the polyelectrolyte provides proton conductivity; a second polymer affords mechanical integrity. Blending usually involves commercially available polymers or inexpensive polymer precursors, which makes it a simple and cost-effective route to produce PEMs. More importantly, the blending approach eliminates the need to optimize the mechanical, chemical and physical properties in a single polymer chain, which renders it a great potential to develop a wide variety of PEMs. However, the blend morphology is crucial since the conducting phase must be continuous for meaningful proton conductivity. Similar with Nafion whose high proton conductivity has been ascribed to the continuous channel morphology when hydrated, analogous bi-continuous blends should also exhibit high proton conductivities.

Selecting the right polyelectrolyte is very critical for blend membranes. The naphthalenic sulfonated polyimides (SPIs) are a widely studied polyelectrolyte system due to their excellent thermal oxidative, chemical, and mechanical stability, high proton conductivity, good film-forming ability, and low methanol and gas permeability.[6,8,18-24] However, SPIs usually tend to swell extensively. Poly(vinylidene fluoride) (PVDF) is an excellent candidate for the hydrophobic host in blend membranes: PVDF is commercially available, chemically and mechanically stable, and can be easily processed into membranes.[25-29] In addition, PVDF based membranes have reduced methanol permeability and swelling ratios, and exhibit good performance in direct methanol fuel cells (DMFC).[29-30] Regardless of the excellent chemical,

thermal, electrical and mechanical properties of SPI and PVDF, the blend of these two materials has rarely been investigated. Herein, we report the blend membranes derived from 100% degree of sulfonation (DS) SPI and PVDF. The SPI was synthesized by direct polymerization of nathphalenic dianhydride and sulfonated diamine monomers. With its 100% DS SPI exhibits excellent proton conductivity, while the rigid PVDF matrix, incompatible with SPI, provides mechanical and dimensional integrity. The membranes' ion exchange capacity (IEC) can be easily modified by varying the ratio of SPI to PVDF. Morphology characterization of PEM cross-sections by TEM reveals micro-phase separation of the two incompatible materials which changed into a bi-continuous system above a percolation threshold of the SPI conetnt in PEMs. Without significant effort in process optimization, the obtained SPI/PVDF blend membrane exhibits higher conductivity than Nafion at the optimal composition, with significant improvement in dimensional stability.

Experimental

Materials

Unless otherwise specified, all chemicals and solvents were ACS reagent grade and used as received from commercial suppliers without further purification. Dimethyl sulfoxide (DMSO) was dried over activated 4 Å molecular sieves, and triethylamine (TEA) and *m*-cresol were distilled before use. 4,4'-Diamino-biphenyl 2,2'-disulfonic acid (BDSA), received from TCI, was purple before purification. BDSA was purified by dissolving in an aqueous TEA solution and then precipitating upon the addition of 1M HCl. The process was repeated until BDSA was obtained as a white solid which was then dried under vacuum at 70 ºC overnight prior to use. Nafion 117, PVDF (M_w = 534,000 Da), and 1,4,5,8-naphthalene tetracarboxylic dianhydride (NTDA) were purchased from Sigma-Aldrich. NTDA and benzoic acid were dried under vacuum at 170 ºC and 60 ºC overnight, respectively, prior to the polycondensation reaction.

Synthesis of sulfonated polyimide (triethyl ammonium salt) (SPI)

Under N_2, BDSA (0.69 g, 2 mmol), TEA (0.7 mL, 5 mmol), and *m*-cresol (6 mL) were added to a 100 mL three-neck round bottom flask and were vigorously stirred with a mechanical stirrer. After the BDSA was completely dissolved at 80 ºC, NTDA (0.53 g, 2 mmol) and benzoic acid (0.34 g, 2.8 mmol) were added. The reaction system was stirred at 80 ºC for 4 h, and then additional *m*-cresol (20 mL) was added to dilute the viscous mixture. The reaction temperature was increased to 180 ºC. After 14 h, the heating was discontinued, DMSO (100 mL) was added, and the system was allowed to cool. The mixture was poured into ethyl acetate (500 mL) to precipitate the polymer. The crude polymer was isolated by filtration and then re-precipitated twice by dissolving the polymer in DMSO (100 mL) and precipitating into ethyl acetate (500 mL). Finally, the SPI was dried under vacuum at 80 ºC overnight (1.1 g).

Film casting

Blend membranes were fabricated by the solvent-casting method. This procedure describes the preparation of 10 mg membranes. Predetermined amounts of PVDF and SPI were dissolved in DMSO in separate vials using magnetic stirring. Each solution was fixed at 0.02 g/mL, and the total mass of SPI and PVDF was 10 mg. The two solutions were combined and stirred until the system was homogeneous. Membranes were solution-cast by adding the mixed solutions drop by drop onto a clean glass plate from ~5 cm height at room temperature, typically covering a full ~4×1 cm^2 area, and carefully dried with infrared heat at ~60 ºC in air. The infrared heat must be uniformly applied to membrane surfaces to avoid inhomogeneous heating and ensure the desired morphology. After ~3 hours, the membrane had turned translucent, and the glass plate was transferred to a vacuum oven at 80 ºC for further drying overnight. The dried membranes (5-15 μm thick) were cut to size (~3×0.5-1 cm^2) and then removed from the substrate by immersing in water. The as-synthesized membranes were soaked in 1 M HCl for 48 h to ensure that all sulfonate groups in the membranes were in their acidic form. The membranes were then washed extensively with water, and prior to conductivity tests, PEMs were stored in Milli-Q water.

Characterization

^{1}H NMR analyses were performed at room temperature in deuterated DMSO on a Varian UnityPlus 500 spectrometer at 500 MHz with the residual solvent proton signals as chemical shift standards. FT-IR spectra were acquired from a Mattson Galaxy 300 spectrometer purged with dry nitrogen, with the signal averaging 128 scans at a resolution of 4 cm^{-1}. All FT-IR samples were dried, mixed with KBr, ground, and then pressed into pellets. Thermogravimetric analyses (TGA) were carried out in air on Perkin-Elmer TGA 7 instruments at a heating rate of 10 ºC/min. TGA samples were dried under vacuum at 80 ºC overnight prior to analysis. Dried samples were held at 120 ºC in the TGA apparatus for 30 min prior to initiating the run. The microstructure of blend membranes was imaged using a JEOL-100CX transmittance electron microscope. To prepare membrane cross-sections for TEM analysis, membranes were immersed in 0.5 M $AgNO_3$ solution overnight to stain the ionic domains by ion exchange of sulfonic acid groups for silver. Samples were rinsed with water, and then dried under vacuum at 80 ºC overnight. The stained membranes were embedded in epoxy resin, dried at 50 ºC for 24 h, and then sectioned with an ultramicrotome to generate ~100 nm-thick slices. The slices were picked up with TEM copper grids.

Conductivity measurements

The membrane proton conductivities were measured with an alternating current (AC) impedance analyzer HP 4192A over the frequency range from 5 Hz to 13 MHz. Membranes were placed between two Pt electrodes in a home-made Teflon cell. The entire setup was kept in Milli-Q water at controlled temperatures for at least 10 min to saturate membranes and impedance was measured in the in-plane direction. From the Nyquist plot, the resistance of the membrane was estimated, and then the membrane proton conductivity was calculated using the electrodes distance and membrane cross-sectional area, as shown in equation (1):

$$\sigma = \frac{L}{R \times A} \quad (1)$$

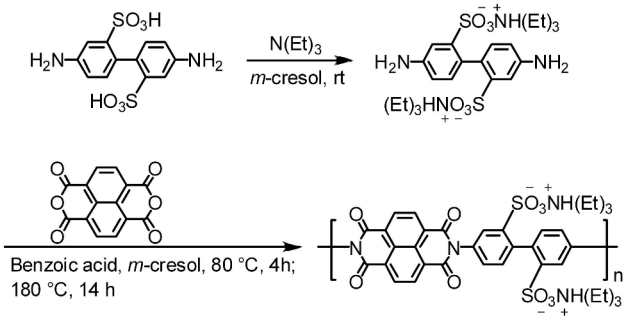

Scheme 1. Synthesis of sulfonated polyimide (triethylammonium salt) (SPI).

Where σ is the membrane proton conductivity, L represents the distance between two electrodes, A stands for the membrane cross-sectional area, and R is the bulk membrane resistance estimated from the Nyquist plot.

Water uptake

The water uptake of membranes was measured gravimetrically. After equilibration in Milli-Q water for two days at room temperature, membranes were removed from water, and weighed after the surface water was quickly removed using a Kim-wipe. Membranes were then dried under vacuum at 50 ºC overnight and the weight of dried membrane was measured. The membrane water uptake was calculated according to equation (2):

$$\text{Water uptake} = \frac{W_{wet} - W_{dry}}{W_{dry}} \times 100\% \quad (2)$$

where W_{wet} stands for the mass of wet membranes and W_{dry} represents the weight of dried membranes.

Dimensional stability

Membranes were saturated in Milli-Q water for two days at room temperature before the dimensions of swollen membrane were measured. After drying under vacuum at 50 ºC overnight, the dried membranes were measured. The swelling ratio was calculated from the length (longest dimension) of the membrane, as shown in equation (3):

$$\text{Swelling ratio} = \frac{L_{wet} - L_{dry}}{L_{dry}} \times 100\% \quad (3)$$

where L_{wet} and L_{dry} represent the lengths of wet and dried membranes, respectively. The uncertainty in the measurement is <3 %.

Theoretic ion exchange capacity (IEC)

The ion exchange capacity (IEC) of membranes was calculated from the molecular weight of SPI repeating unit and SPI weight content in each membrane. The IEC was calculated as shown in equation (4):

$$\text{IEC} = \frac{m_{H^+}}{W_{dry}} \quad (4)$$

where m_{H+} expresses the quantity of sulfonic acid groups.

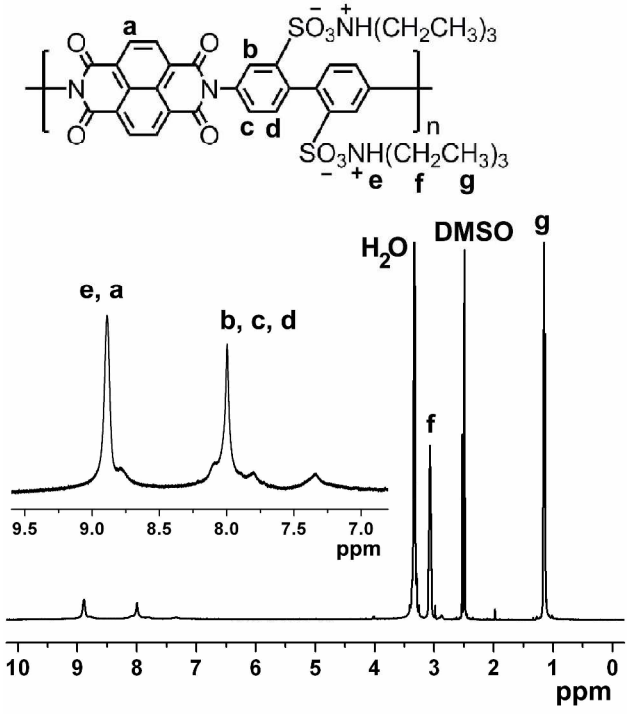

Fig. 1 500 MHz ^{1}H NMR spectrum of SPI.

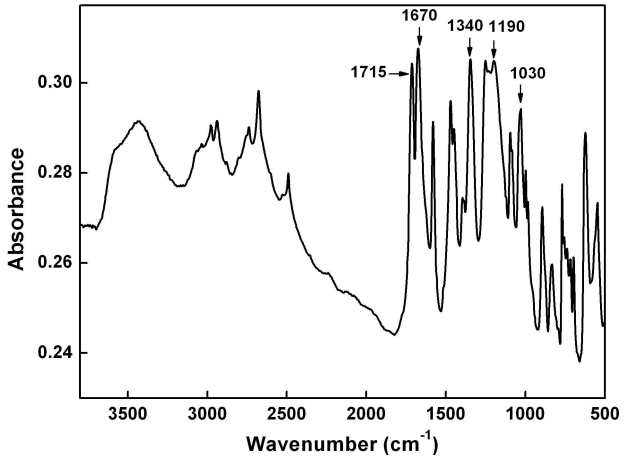

Fig. 2 FT-IR spectrum of SPI. The sample was made into a pellet with KBr.

Results and Discussion

Synthesis and characterization of SPI

SPI was synthesized by step growth polymerization of BDSA and NTDA as illustrated in Scheme 1.[31] Using the sulfonated diamine monomer avoided the drawbacks associated with "post-sulfonation" method, which usually results in low sulfonation degrees, cross-linking, and polymer chain degradation.[18]

The chemical structure of SPI was confirmed by ^{1}H NMR spectroscopy (Fig. 1). Proton peaks from the ethyl groups at ~1.1 and 3.0 ppm confirmed the presence of the triethylammonium moiety in the polymer. Peaks at 8.7-8.8 ppm were assigned to the naphthalenic and ammonium protons, while the peaks at 7.35, 7.8, and 8.0 ppm were attributed to phenylene protons in the BDSA polymer segments.[7]

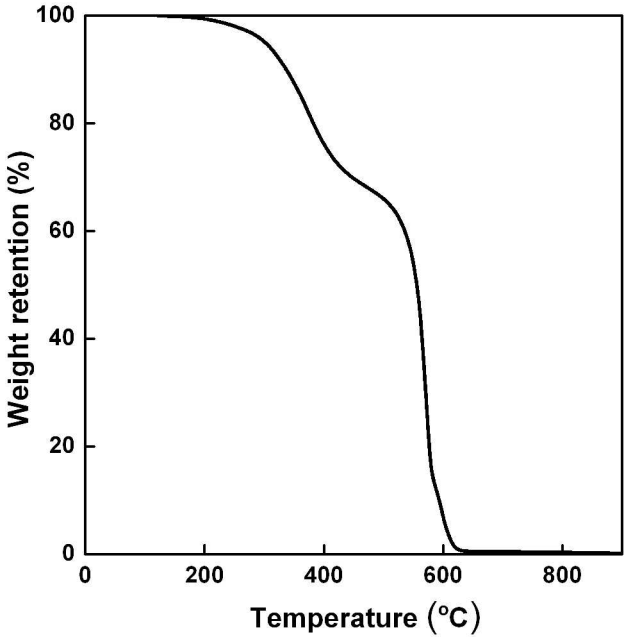

Fig. 3 Thermogravimetric analysis of SPI, run at a heating rate of 10 ºC/min in air.

FT-IR spectroscopy verified the SPI structure (Fig. 2). The spectrum showed strong and broad O–H stretching bands at 3435 cm^{-1} due to water absorbed by the hygroscopic polymer. Bands between 3200 cm^{-1} and 3000 cm^{-1} were assigned to aromatic C–H stretching while bands from 3000 cm^{-1} to 2900 cm^{-1} resulted from aliphatic C–H stretching of the triethylammonium moiety. The characteristic C=O symmetric and antisymmetric stretching bands at 1715 cm^{-1} and 1670 cm^{-1}, and the C–N–C bending mode at 1340 cm^{-1} confirmed the presence of the naphthalenic imide. In addition to the characteristic peaks at high wavenumbers, the SPI structure was supported by the S=O antisymmetric and S=O symmetric stretching bands at 1190 cm^{-1} and 1030 cm^{-1}, respectively. The absence of the characteristic peak at 1780 cm^{-1} for a polyamic acid indicated a high degree of imidization.

Thermogravimetric analysis (TGA) was performed to investigate the thermal stability of SPI. As presented in Fig. 3, there are two major weight loss events. The first weight loss (~30 %) commenced at ~200 ºC and continued to 400 ºC which is likely due to desulfonation.[31] The weight loss observed above 400 ºC corresponds to the oxidative degradation of the aromatic backbone of the polymer.

Fabrication and characterization of PEMs from the blending of SPI and PVDF

The synthesized SPI is soluble in aprotic solvents (for example, NMP and DMSO) and *m*-cresol. Blend PEMs were obtained by solution-casting a DMSO mixture of SPI and PVDF onto flat glass surfaces. Once soaked in water, the dried membrane samples were easily peeled from the glass substrate, and after acidification, the membranes had a yellow color. Table 1 summarizes the composition and experimental results from the blend membranes.

Water uptake and proton conductivity

A key parameter of PEMs is water absorption. Membranes

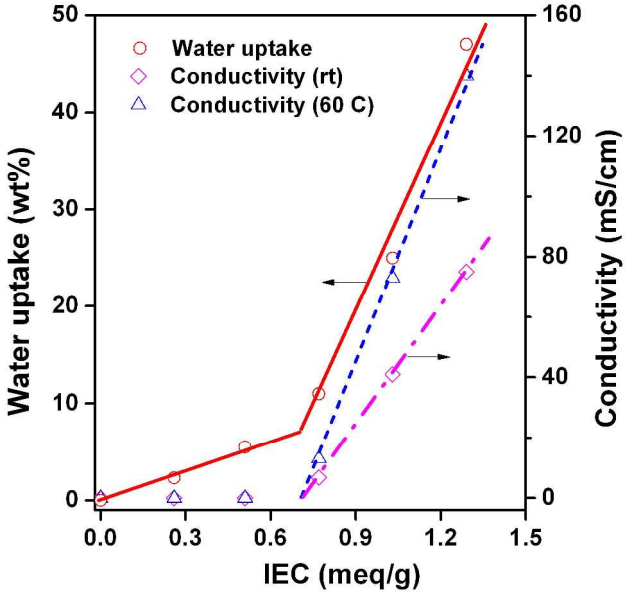

Fig. 4 Blend membrane proton conductivity and water uptake as a function of membrane IEC. (The lines are a guide to the eye).

require water to dissociate SO_3H groups and act as "vehicles" to transport protons from the anode to the cathode; however, too much water usually results in severe swelling and poor mechanical strength. Ideally, the water uptake facilitates high proton conductivity without sacrificing a membrane's mechanical properties. The ion exchange capacity (IEC), expressed as mmol acid/g of sample, defines the number of charge carriers in a membrane and is directly correlated to a membrane's ability to absorb and retain water. As shown in Fig. 4, membrane water uptake increased linearly with SPI contents up to about 0.72 meq/g (~28 wt% SPI). However, beyond this value, water uptake increased drastically, indicating a change in the membrane morphology.[32] Since PVDF is hydrophobic, the SPI phase is primarily responsible for water absorption. When the SPI content in blend membranes is low, most sulfonic acid groups are isolated in ionic clusters distributed throughout the continuous PVDF matrix, and water may be accessible to only a few clusters. As the SPI content increases, accessible ionic clusters either increase in size or link to adjacent clusters, increasing the measured water uptake. When the SPI content in blend membranes exceeded ~30 wt%, the membrane morphology of isolated ionic clusters in PVDF transformed to a bi-continuous network of water swollen channels in a PVDF matrix. Above the apparent 30 wt% percolation threshold, water uptake increased linearly, but at a higher rate. Not surprisingly, a pure PVDF membrane (IEC = 0) had zero water absorption.

Proton conductivity is one of the most important parameters for evaluating the performance of PEMs as well as the practicability of fuel cells. It is widely accepted that the proton conductivity of PEMs is strongly related to the number of charge carriers (H^+), so an ideal membrane would have a high sulfonic acid content without sacrificing the PEMs' mechanical properties. The conductivity tests were conducted with the cell submersed in Milli-Q water (100 % RH), and proton conductivities were measured for the series of blend membranes as a function of membrane IEC (Fig. 4). Pure PVDF membranes (IEC = 0) and

Table 1 Summary of SPI/PVDF membrane characteristics.

SPI wt% in PEMs	IEC (meq/g)	Conductivity at rt (mS/cm)	Conductivity at 60 °C (mS/cm)	Swelling ratio (%)	Water uptake (wt%)
0	0[a]	0	0	<3	0
10	0.26[a]	0	0	<3	2
20	0.51[a]	0	0	<3	6
30	0.77[a]	7	13	<3	11
40	1.03[a]	41	73	<3	25
50	1.29[a]	75	140	<3	47
Nafion 117[b]	0.91[4]	62	110	18[4]	21

[a]IEC values were calculated from the SPI repeating unit (M_n = 778 g/mol) and the composition of blend membranes.
[b]Nafion 117 was included for comparison.

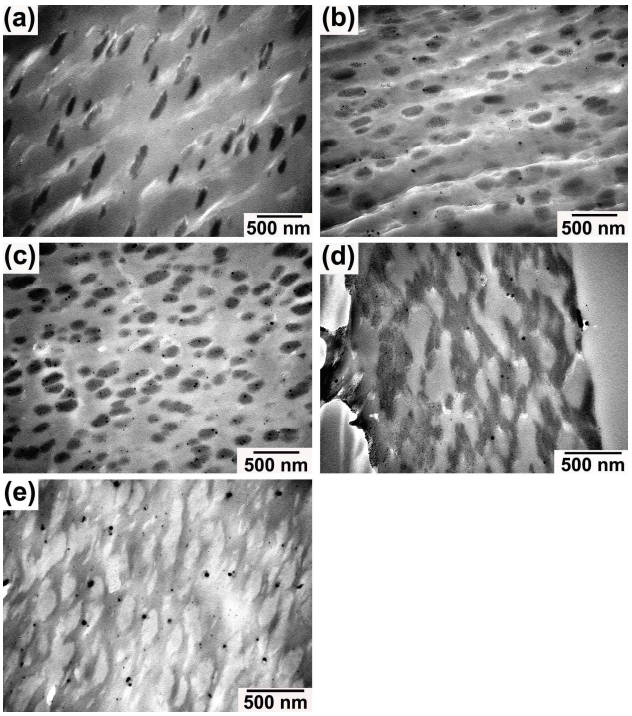

Fig. 5 Cross-sectional TEM images of blend membranes with different SPI contents: (a) 10 wt%; (b) 20 wt%; (c) 30 wt%; (d) 40 wt%; and (e) 50 wt%.

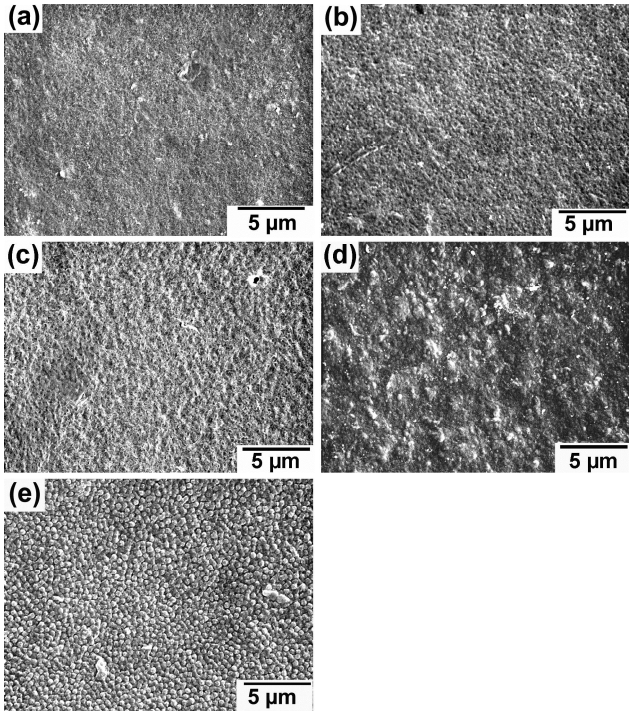

Fig. 6 Surface SEM images of blend membranes with different SPI contents: (a) 10 wt%; (b) 20 wt%; (c) 30 wt%; (d) 40 wt%; and (e) 50 wt%.

blend membranes with an IEC value < 0.72 meq/g had no measurable proton conductivity, which is consistent with the isolated ionic clusters assumption. Beginning at IEC of 0.77 meq/g (30 wt% SPI), the presumed percolation threshold, proton conductivity increased linearly from 7 to 75 mS/cm (50 wt% SPI) at room temperature.

The proton conductivity of Nafion 117 was measured as a control for conductivity experiments (Table 1). At room temperature, the conductivity of Nafion 117 was 62 mS/cm, which is reasonably close to the reported conductivity data (60 mS/cm).[33] The proton conductivity of a 50 wt% SPI blend PEM was higher than Nafion 117 at both room temperature and 60 ºC. The high conductivity of the blend membranes might be due to continuous proton conducting SPI phase separated from the hydrophobic PVDF analogous to Nafion 117.[34]

The proton conductivities of both blend membranes and Nafion 117 were relatively low at room temperature but increased rapidly as the temperature was raised to 60 ºC. The elevation of temperature might have stimulated the dynamics of proton transport and structural reorganization, which favors fast proton conduction.[35] Moreover, temperature increase might activate both the proton diffusion and molecular diffusion leading to improved proton conductivities at high temperatures.[35]

Microstructure of blend PEMs

The nature of acid groups, chemical composition, and membrane microstructure all contributes to the properties of PEMs. To obtain direct morphologic information, ~100 nm-thick cross-sectional slices of blend membranes were analyzed by TEM. Fig. 5 displays images of SPI/PVDF blend membranes with different blending ratios. After staining with Ag+, the SPI appears as dark regions, while the matrix material, PVDF, is brighter. A phase-separated morphology was seen for all compositions. Blend membranes with 10-30 wt% SPI show randomly distributed ionic domains; the domain size seems constant, but the areal density of domains increases with SPI contents. TEM images of membranes

with >30 wt% SPI content show ionic domains interconnected into a continuous network. The images in Figs. 5c and 5d provide direct evidence for a percolation phenomenon near 30 wt% SPI. The TEM image of the membrane with 40 wt% SPI content shows an apparent bi-continuous morphology with conducting paths for proton transport, which is consistent with the conductivity and water uptake studies. The ionic domains have sizes of 30-100 nm. A finer phase-separated morphology was found in the 50 wt% SPI blend membrane, and the domain size dropped to 20-40 nm. The constant ionic domain size of blend membranes with 10-30 wt% SPI might be due to independent aggregation of SPI in PVDF matrix. Above the percolation threshold the isolated ionic domains interconnect causing possible domain size increase. However, when there is sufficient amount of SPI the ionic domains can be easily bridged during solvent evaporation before domain size grows resulting in denser but smaller domain sizes, which might explain the drop of ionic domain size from blend membrane with 40 wt% SPI content to 50 wt% SPI. Scattered black dots seen in most images are likely silver oxide clusters generated through the photolysis of silver nitrate, which was applied for staining blend membranes. However, once the SPI content reached 60 wt% the resulting membranes became brittle, which might be due to the reduced continuity of the PVDF phase with increased SPI content. While the cross-sectional TEM images provide direct evidence for a phase-separated structure in dried membranes, water saturated membranes might have different ionic domain sizes or domain connections.

As PEMs are used as not only a proton conductor but also a separator to prevent the mixing of fuels with the oxidant, PEMs cannot have pin holes, which will allow permeation of fuels. We used SEM to obtain the surface microstructure of blend membranes that had been kept in water for over a week, and then dried (Fig. 6). No holes were seen for any compositions. The SEM image of the membrane with 10 wt% SPI content showed a homogeneous surface structure. The roughness of the blend membrane surfaces increased with the SPI contents. The image in Fig. 6e showed a spherical morphology in a 50 wt% SPI membrane. It is noteworthy that the SEM images were taken from the blend membranes which had been kept in water for over a week, suggesting that blend PEMs were hydrolytically stable.

Swelling properties

High proton conductivity and minimal swelling properties are highly desirable for PEMs. Membrane dimensional stability was characterized by measuring the dimensional changes between the dry and water saturated states which are usually reported by either membrane length or area or volume changes.[36-37] Membranes that swell excessively can detach from the electrode surfaces as most electrodes do not swell, resulting in mechanical stress.[38] As illustrated in Table 1, Nafion 117 equilibrated in water increased 18 % in length compared to the dry film and similar swelling behavior was observed for the width direction. On the contrast, no measurable changes in membrane dimensions were observed for the blend membrane systems and the reported <3 % swelling ratio in length was estimated from the experimental error. In order to avoid generating more error during calculation for area or volume, the dimensional change in membrane length was used for calculating the swelling ratio. The severe expansion of Nafion 117 explains its poor performances in direct methanol fuel cells (DMFCs), as the permeability of Nafion to methanol is related to the high swelling of Nafion in water. The very low water swelling behavior of the blend membranes may be due to the rigid matrix of crystalline PVDF which suppressed the water swelling of SPI in hydrated membranes. It has been reported that most SPI based proton exchange membrane systems have low methanol permeability.[18] The as-synthesized blend PEMs should have advantages over Nafion in methanol cross-over due to much less swelling in water.

Conclusions

A SPI with 100 % DS was prepared by the direct polycondensation reaction of a naphthalenic dianhydride monomer and a sulfonated diamine monomer. A series of PEMs were prepared by blending SPI with PVDF followed by acidification, of which the PEM with 50 wt% of SPI content revealed higher proton conductivity than Nafion 117. A percolation phenomenon was observed when the weight content of SPI in PEM reached 30 % where both proton conductivity and water uptake drastically increased and then stayed proportional to the weight fraction of SPI. The 30 wt% percolation threshold was also confirmed by TEM cross-sectional images which showed densely scattered ionic domains getting connected. A bi-continuous morphology was observed in PEMs with 40 wt% and 50 wt% SPI. In addition, the blend membranes showed a high dimensional stability. This blend PEM system should also be more cost effective compared to Nafion due to much easier synthesis and film processing.

Acknowledgements

The authors thank Michigan State University (MSU) for financial support of this research. The authors also thank MSU chemistry department Dan Holmes for the help with ^{1}H NMR and Kathy Severin for her help with FT-IR, and Alicia Pastor from MSU Center for Advance Microscopy for the help with TEM.

Notes and references

[a] *Department of Chemistry, Michigan State University, East Lansing, MI 48824, USA; Tel: 01-517-355-9715; E-mail: yuanqin9912@gmail.com*
[b] *IBM Corporation: 2070 Rt 52, Hopewell Junction, NY 12533, USA*
[c] *Owens-Illinois Incorporation: 1 Michael Owens Way, Perrysburg, OH 43551, USA*
[d] *Deceased October 18, 2012*

1. Y. L. Liu, *Polym. Chem.*, 2012, **3**, 1373-1383.
2. K. A. Mauritz and R. B. Moore, *Chem. Rev.*, 2004, **104**, 4535-4585.
3. C. J. Zhao, X. F. Li, Z. Wang, Z. Y. Dou, S. L. Zhong and H. Na, *J. Membr. Sci.*, 2006, **280**, 643-650.
4. C. Chuy, J. F. Ding, E. Swanson, S. Holdcroft, J. Horsfall and K. V. Lovell, *J. Electrochem. Soc.*, 2003, **150**, E271-E279.
5. H. L. Cheng, J. M. Xu, L. Ma, L. S. Xu, B. J. Liu, Z. Wang and H. X. Zhang, *J. Power Sources*, 2014, **260**, 307-316.
6. T. Nakano, S. Nagaoka and H. Kawakami, *Polym. Adv. Technol.*, 2005, **16**, 753-757.
7. H. Y. Pan, Y. Y. Zhang, H. T. Pu and Z. H. Chang, *J. Power Sources*, 2014, **263**, 195-202.
8. W. Li, X. X. Guo and J. H. Fang, *J. Mater. Sci.*, 2014, **49**, 2745-2753.

9. Y. S. Yang, Z. Q. Shi and S. Holdcroft, *Macromolecules*, 2004, **37**, 1678-1681.
10. Y. Chen, J. R. Rowlett, C. H. Lee, O. R. Lane, D. J. VanHouten, M. Q. Zhang, R. B. Moore and J. E. McGrath, *J. Polym. Sci. Pol. Chem.*, 2013, **51**, 2301-2310.
11. J. N. Ren, S. L. Zhang, Y. Liu, Y. Wang, J. H. Pang, Q. H. Wang and G. B. Wang, *J. Membr. Sci.*, 2013, **434**, 161-170.
12. E. M. W. Tsang, Z. Zhang, Z. Shi, T. Soboleva and S. Holdcroft, *J. Am. Chem. Soc.*, 2007, **129**, 15106.
13. E. F. Abdrashitov, V. C. Bokun, D. A. Kritskaya, E. A. Sanginov, A. N. Ponomarev and Y. A. Dobrovolsky, *Solid State Ionics*, 2013, **251**, 9-12.
14. Y. C. Shu, F. S. Chuang, W. C. Tsen, J. D. Chow, C. Gong and S. Wen, *J. Appl. Polym. Sci.*, 2008, **108**, 1783-1791.
15. M. L. Di Vona, E. Sgreccia, S. Licoccia, M. Khadhraoui, R. Denoyel and P. Knauth, *Chem. Mat.*, 2008, **20**, 4327-4334.
16. H. L. Wu, C. C. M. Ma, F. Y. Liu, C. Y. Chen, S. J. Lee and C. L. Chiang, *Eur. Polym. J.*, 2006, **42**, 1688-1695.
17. J. V. Gasa, R. A. Weiss and M. T. Shaw, *J. Polym. Sci. Pt. B-Polym. Phys.*, 2006, **44**, 2253-2266.
18. M. A. Hickner, H. Ghassemi, Y. S. Kim, B. R. Einsla and J. E. McGrath, *Chem. Rev.*, 2004, **104**, 4587-4611.
19. B. R. Einsla, Y. S. Kim, M. A. Hickner, Y. T. Hong, M. L. Hill, B. S. Pivovar and J. E. McGrath, *J. Membr. Sci.*, 2005, **255**, 141-148.
20. Y. Okazaki, S. Nagaoka and H. Kawakami, *J. Polym. Sci. Pt. B-Polym. Phys.*, 2007, **45**, 1325-1332.
21. L. Zou and M. Anthamatten, *J. Polym. Sci. Pol. Chem.*, 2007, **45**, 3747-3758.
22. H. S. Lee, A. S. Badami, A. Roy and J. E. McGrath, *J. Polym. Sci. Pol. Chem.*, 2007, **45**, 4879-4890.
23. H. L. Wu, C. C. M. Ma, C. H. Li, T. M. Lee, C. Y. Chen, C. L. Chiang and C. Wu, *J. Membr. Sci.*, 2006, **280**, 501-508.
24. N. Asano, K. Miyatake and M. Watanabe, *J. Polym. Sci. Pol. Chem.*, 2006, **44**, 2744-2748.
25. W. H. Choi and W. H. Jo, *J. Power Sources*, 2009, **188**, 127-131.
26. A. Mokrini and M. A. Huneault, *J. Power Sources*, 2006, **154**, 51-58.
27. P. Piboonsatsanasakul, J. Wootthikanokkhan and S. Thanawan, *J. Appl. Polym. Sci.*, 2008, **107**, 1325-1336.
28. A. Mokrini, M. A. Huneault and P. Gerard, *J. Membr. Sci.*, 2006, **283**, 74-83.
29. H. Y. Jung and J. K. Park, *Electrochim. Acta*, 2007, **52**, 7464-7468.
30. S. N. Xue and G. P. Yin, *Polymer*, 2006, **47**, 5044-5049.
31. C. Genies, R. Mercier, B. Sillion, N. Cornet, G. Gebel and M. Pineri, *Polymer*, 2001, **42**, 359-373.
32. M. J. Sumner, W. L. Harrison, R. M. Weyers, Y. S. Kim, J. E. McGrath, J. S. Riffle, A. Brink and M. H. Brink, *J. Membr. Sci.*, 2004, **239**, 199-211.
33. J. J. Fontanella, M. G. McLin, M. C. Wintersgill, J. P. Calame and S. G. Greenbaum, *Solid State Ionics*, 1993, **66**, 1-4.
34. K. Schmidt-Rohr and Q. Chen, *Nat. Mater.,* 2008, **7**, 75-83.
35. W. Jang, S. Sundar, S. Choi, Y. G. Shul and H. Han, *J. Membr. Sci.*, 2006, **280**, 321-329.
36. D. Zhao, J. H. Li, M. K. Song, B. L. Yi, H. M. Zhang and M. L. Liu, *Adv. Energy Mater.,* 2011, **1**, 203-211.
37. J. S. Yang, Q. F. Li, L. N. Cleemann, J. O. Jensen, C. Pan, N. J. Bjerrum and R. H. He, *Adv. Energy Mater.,* 2013, **3**, 622-630.
38. D. Liu and M. Z. Yates, *J. Membr. Sci.*, 2009, **326**, 539-548.

Sulfonated Polyimide and PVDF Based Blend Proton Exchange Membranes for Fuel Cell Applications

Blend proton exchange membranes were prepared from sulfonated polyimide and PVDF and a percolation threshold of 30wt% SPI was observed.

Qin Yuan,* Ping Liu, and Gregory L. Baker